

RESEARCH ARTICLE

Estimating methane emissions from underground natural gas pipelines using an atmospheric dispersion-based method

Shanru Tian¹, Kathleen M. Smits^{2,*}, Younki Cho^{1,3}, Stuart N. Riddick³, Daniel J. Zimmerle^{3,4}, and Aidan Duggan³

Methane (CH₄) leakage from natural gas (NG) pipelines poses an environmental, safety, and economic threat to the public. While previous leak detection and quantification studies focus on the aboveground infrastructure, the analysis of underground NG pipeline leak scenarios is scarce. Furthermore, no data from controlled release experiments have been published on the accuracy of methods used to (1) quantify emissions from an area source and (2) use these emissions to quantify the size of a subsurface leak. This proof-of-concept work uses CH₄ mole fraction, as measured by a single gas sensor, as an input to a simple dispersion-based model (WindTrax) under ideal conditions (i.e., in a field) and compares the calculated emissions to the known controlled NG release rates. The aboveground and surface CH₄ mole fractions were measured for 5 days at a field testbed using controlled underground release rates ranging from 0.08 to 0.52 kg hr⁻¹ (3.83–24.94 ft³ hr⁻¹). Results confirmed that the mean normalized CH₄ mole fraction increases as the atmosphere transitions from the Pasquill–Gifford (PG) stability class A (extremely unstable) to G (extremely stable). The estimated surface CH₄ emissions showed large temporal variability, and for the emission rates tested, at least 6 h of data are needed to have a representative estimate from subsurface pipeline leaks ($\pm 27\%$ of the controlled release rate on average). The probability that the emission estimate is within $\pm 50\%$ of the controlled release rate ($P_{\pm 50\%}$) is approximately 50% when 1 h of data is collected; the probability approaches 100% with 3–4 h of data. Findings demonstrate the importance of providing enough data over time for accurate estimation of belowground leak scenarios. By adopting the estimation method described in this study, operators can better estimate leakage rates and identify and repair the largest leaks, thereby optimizing annual greenhouse gas emissions reductions and improving public safety.

Keywords: Methane emissions, Gas distribution, Natural gas leak detection and quantification, Pipeline leakage, Atmospheric stability

1. Introduction

Fugitive methane (CH₄) emissions from natural gas (NG) pipelines pose an ongoing threat to the environment and public safety. Common causes of pipeline leakage include corrosion, incorrect operation due to human error, excavation or similar ground disturbances, natural force damage caused by ground shifts or aboveground loads, and equipment failure (Pipeline and Hazardous Materials

Safety Administration [PHMSA], 2018). Pipeline leakage events result in significant safety issues. From 2000 to 2019, the PHMSA reported pipeline incidents resulting in 202 fatalities, 918 injuries, and an estimated total cost of \$2.94 billion (PHMSA, 2022). It is estimated that CH₄ emissions from NG distribution main leaks are 0.69 Tg per year, accounting for 7.6% of the total U.S. CH₄ emissions (Weller et al., 2020). CH₄ emissions from the NG distribution networks contribute to 56% of the total estimated CH₄ emissions in Paris (Defratyka et al., 2021). Given that the global warming potential of CH₄ is 84 times greater than that of CO₂ over a 20-year horizon (Intergovernmental Panel on Climate Change, 2014), the environmental benefits of NG as a short-term approach for mitigating climate change would be negated if CH₄ emissions in the NG supply chain exceed 3.2% of total NG production (Alvarez et al., 2012; United Nations Framework Convention on Climate Change, 2022). Typically, local NG distribution companies detect atmospheric CH₄ mole fraction

¹ Department of Civil Engineering, The University of Texas at Arlington, Arlington, TX, USA

² Department of Civil and Environmental Engineering, Southern Methodist University, Dallas, TX, USA

³ The Energy Institute, Colorado State University, Fort Collins, CO, USA

⁴ Department of Mechanical Engineering, Colorado State University, Fort Collins, CO, USA

* Corresponding author:
Email: kathleen.smits@uta.edu

from underground leaks using vehicle and walking surveys (PHMSA, 2017). However, studies showed that NG pipeline leaks are difficult to locate and quantify from the above-ground observations due to limited understanding of (1) how CH₄ accumulates or disperses in the atmosphere under different environmental conditions and (2) the underground CH₄ transport and surface manifestation of such leaks (Okamoto and Gomi, 2011; Mitton, 2018; National Association of Regulatory Utility Commissioners, 2019; Cho et al., 2020). Therefore, a better understanding of the influence of atmospheric conditions on the above-ground CH₄ plume from underground leaks is required to improve leak detection and quantification and risk assessment.

NG distribution pipelines are surveyed by distribution companies through routine inspection. Once a leak is discovered, it is classified based on the existing or probable hazard to the person and property (Hendrick et al., 2016; Washington Administrative Code, 2019). Generally, Grade 1 leaks are prioritized for immediate repair. Grade 2 and 3 leaks are classified as nonhazardous based on location, CH₄ magnitude, and potential for migration of the leaked gas. Grade 2 and 3 leaks require repair within 12–15 months of detection and then reevaluation after 15 months of discovery. Before repair, unresolved Grade 2 and 3 leaks require periodic inspection.

Despite repeated observation, leak classification does not consider the effects of environmental conditions on the magnitude of the measured CH₄ mole fraction. A recent vehicle survey in Durham, NC, showed that leak detection density was 50% higher at night (0.33 leaks per mile) compared to daytime conditions (0.22 leaks per mile) when following the same route (Gallagher et al., 2015). Therefore, many underground leaks may go undetected using current survey criteria that fail to incorporate the effects of environmental conditions on leak detection.

Previous studies have used several methods to estimate emissions from underground NG pipeline leaks, including bottom-up, local level methods, such as the surface dynamic chamber method (Lamb et al., 2015; Hendrick et al., 2016; Zimmerle et al., 2017), downwind tracer-ratio methods (Lamb et al., 2015; Weller et al., 2018), and vehicle-based statistical methods (Von Fischer et al., 2017; Weller et al., 2018; Weller et al., 2020). Enclosing a surface area to measure the CH₄ enhancement, the surface dynamic chamber method relies on knowledge of the flow of air through a controlled chamber volume (National Academies of Sciences, 2018; Riddick et al., 2020). The surface enclosure area is typically 1 m² in size with measurement times in the range of minutes (National Academies of Sciences, 2018) or a series of gridded enclosure placements to overcome the spatial limitations (Lamb et al., 2015). The main shortcoming of this method is that the surface CH₄ expression from underground pipeline leaks has been documented to migrate 2–6 m from the leak location, depending upon the leak size and environmental conditions, such as soil properties and moisture (Okamoto and Gomi, 2011; Ulrich et al., 2019; Cho et al., 2020; Cho et al., 2022), and the chamber may not capture all emitted gas. In addition, recent work by Riddick et al.

(2021) documents the temporal variability in the surface CH₄ expression above an NG pipeline leak. The authors identify variations in wind speed, roughness length, and atmospheric stability as the key environmental variables most significantly affecting the surface CH₄ mole fraction. Cho et al. (2022) measured this change continuously over 4 days for 2 different known leakage rates, demonstrating how it varies by over 100%, depending on the time of day. Downwind tracer-ratio methods are often used as a supplementary quality assurance method to evaluate the performance of other methods, such as the surface chamber method (Lamb et al., 2015). Such methods require accurate knowledge of the known leak location and are sensitive to environmental conditions, such as wind and the accurate co-placement of the tracer release and leak site (Mønster et al., 2019). Vehicle-based methods estimate emissions using a statistically fitted linear model with the maximum CH₄ mole fraction, the total plume peak area, and the ratio of maximum CH₄ mole fraction to peak area (Von Fischer et al., 2017). Although this method shows promise for city or regional studies, it relies on statistical analysis and does not incorporate the impacts of atmospheric conditions on the dispersion of the CH₄ plume. When compared with surface chamber estimates, vehicle-based statistical estimates show larger emission estimates with very few indications of ground truth estimates from known underground leak rates (Weller et al., 2018).

As few of the above approaches have been verified using controlled underground releases, evaluating their accuracy remains an open challenge, and therefore, CH₄ emissions from pipeline systems remain poorly characterized. To the authors' knowledge, there have been no studies to date that investigate the effects of time-varied weather conditions on emission estimate accuracy from subsurface pipeline leaks in controlled conditions. Comparing a method's emission estimates to known, controlled underground release over a range of environmental and operating conditions is the first step toward method validation.

Atmospheric dispersion models have been used to inversely calculate gas emissions across a wide range of scales, spanning from the microscale to the continental scale (Flesch et al., 2004; Jeong, 2011; Bonifacio et al., 2013; Barkley et al., 2017). The application considered here relies on simple downwind measurements and could be readily applied to open field environments free from obstructions, such as buildings, parked vehicles, and trees. Such conditions are typically seen in upstream sectors, such as gathering and flowlines or in the downstream sector in rural environments or along open extents. For these scenarios that represent short-range dispersion (1 km or less), the inverse dispersion model WindTrax has reported an accuracy of $\pm 10\%$ for emission estimates from agricultural sources (i.e., feedlots, pastures, and farms), landfills, and natural sources (Laubach and Kelliher, 2005; Yang et al., 2017; Riddick et al., 2018). As this method is not limited to specific source sizes and shapes, it allows for flexibility in sensor placement and therefore has good potential for use in estimating CH₄ emissions from NG pipeline leakage scenarios (Riddick et al., 2019).

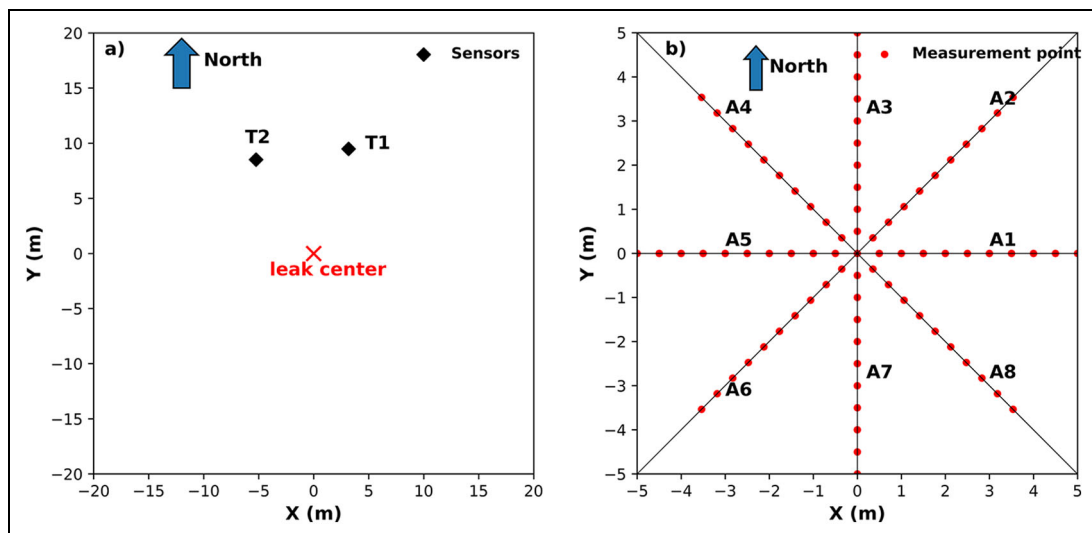


Figure 1. Plan views of the above ground and surface measurement locations relative to the natural gas leak location. (a) The aboveground sensor to measure the atmospheric methane (CH_4) was located at T1 for the first three experiments and T2 for the fourth experiment, due to a change in the predominant wind direction. (b) The gridded layout represents the surface CH_4 measurement locations. In each direction, each point is 0.5 m apart with direction spaced by 45° .

This study explores the effectiveness of using limited surface and aboveground CH_4 mole fraction data as inputs to a near-field dispersion model to calculate CH_4 emissions from subsurface pipeline leaks under realistic conditions. Explicitly, this study aims to (1) link the variations in atmospheric CH_4 mole fraction magnitude to variations in atmospheric stability under a range of controlled NG leak rates, (2) test the accuracy of an inverse modeling approach to estimate emissions by comparing estimates directly against known, controlled underground leak rates, and (3) understand and quantify how much data are needed to estimate emissions within $\pm 50\%$ of controlled leak rates. To our knowledge, this is the first study of its kind to test the emission estimate accuracy against the known rates for belowground pipeline scenarios. Currently, pipeline operators use surface CH_4 measurements to infer the size of a leak and prioritize repair. By adopting the method described in this study to correctly estimate leak rate, operators can estimate emissions and therefore optimize repair and greenhouse gas (GHG) emission reductions.

2. Materials and methods

2.1. Experimental testbed/setup

Field experiments were conducted at the Methane Emission Technology Evaluation Center (METEC) field site, Colorado State University, Colorado. The METEC site includes an underground pipeline testbed that simulates the behavior of pipeline leaks using controlled NG releases under varied subsurface, surface, and atmospheric conditions. Details of the testbed design can be found in Mitton (2018), Ulrich et al. (2019), Cho et al. (2020), and Gao et al. (2021) and will be summarized here. For this work, a testbed simulating a rural right of way with grassy surface cover was selected. The testbed consists of stainless-steel tubing (0.635 cm, model SS-T4-S-035-20, Swagelok, Solon, OH, USA) installed at 0.9 m

below the ground surface along the east-west direction of the site, configured to release compressed NG at specific rates and locations. The tubing runs adjacent to a 10-cm diameter polyvinylchloride pipe to simulate a realistic underground pipeline. The pipeline is back-filled with native soil, classified previously as sandy loam, according to the U.S. Department of Agriculture Soil Texture Classification. The trench is slightly less compact than the surrounding undisturbed soil as discussed in Ulrich et al. (2019). NG (87 ± 2 vol % CH_4) was injected through the stainless-steel tubing into the testbed from an aboveground 145-L compressed NG tank. The gas release rate (reported at kg hr^{-1} of CH_4) was controlled by pressure regulators, solenoid valves, and choked flow orifices and measured using a thermal mass flow meter (range: 0–0.66 kg hr^{-1} , accuracy: $\pm 1\%$, Omega FMA1700 series). Gas was released to the soil through a stainless-steel mud dauber (0.635 cm, model SS-MD-4, Swagelok, USA) with a 10-cm wire mesh cube filled with gravel to prevent clogging.

CH_4 mole fractions were collected at two elevations, 1 m above the ground and at the ground surface. The aboveground CH_4 mole fractions were measured at two separate locations, depending on the experiment (Figure 1a). For the first three experiments (June 1 8:00 AM to June 4 8:00 AM), a trace gas analyzer (Picarro Inc., Santa Clara, CA, USA, G2210, precision: <0.1 ppb) was positioned at location T1 to measure the CH_4 mole fraction at a distance of 10 m from the leak center and 1 m above the ground surface. The measurement interval was approximately 0.8–1 Hz. The analyzer was moved to location T2, located 10 m from the leak center, for the last experiment (June 4 8:00 AM to June 5 8:00 AM) with the same measurement height as the predominant wind direction changed during this period.

Surface CH_4 was measured at the ground surface at 80 locations (Figure 1b) to determine the plume shape and

Table 1. Background methane (CH₄) mole fraction (1-m above ground, 10 m from the leak source) and surface expression area for Experiments 1–4

Experiment	Background CH ₄ Mole Fraction at 1 m (ppm)	Surface Expression Area (m ²)
1	1.89 (±.004)	7
2	1.90 (±.006)	13
3	1.92 (±.042)	20
4	1.88 (±.002)	20

Standard deviations from the background CH₄ mole fraction are noted in parentheses.

size using a handheld CH₄ detector (Bascom Turner Instruments Inc., Norwood, MA, USA, VGI-201 Gas-Rover, resolution: 1.0 ppm, detection limit: approximately 5.0 ppm). The surface CH₄ mole fraction was measured during the last 1 h of each experiment following the method used in a previous study (Cho et al., 2022). In accordance with the manufacturer's procedures, at each measurement point (**Figure 1b**), the rubber cup of the detector was lightly pressed onto the ground surface for 30 s. CH₄ mole fraction was averaged over this time. To ensure that most of the surface expression was recorded, measurements were carried out from the leak center in each direction, A1–A8, until the instrument's detection limit (approximately 5.0 ppm) was reached.

Two meteorological sensors were deployed to continuously measure wind speed, wind direction, solar radiation, and air temperature with a time resolution of 1 min (Figure S1). The first meteorological sensor (METER Group Inc., Pullman, WA, USA, ATMOS41, accuracy: 3% and ±5° for wind speed and direction, respectively; solar radiation: ±5%; air temperature: ± 0.6°C; air pressure: ±0.1 kPa from –10°C to 50°C, ± 0.5 kPa from –40°C to 60°C) was co-placed with the trace gas analyzer at T1 (1 m height). The second sensor (YOUNG Model 81000 Ultrasonic Anemometer, accuracy: wind speed: ±1% ±0.05 m s⁻¹ [0–30 m/s] and ±3% [30–40 m s⁻¹]; wind direction: ±2° [1–30 m s⁻¹] and ±5° [30–40 m s⁻¹]) was a fixed station installed at 6 m above ground, located 76.2 m northwest of the leak center.

2.2. Experiment procedure

Four 24-h experiments were conducted with controlled release rates of 0.08, 0.18, 0.27, and 0.52 kg hr⁻¹ of CH₄ (3.83, 8.64, 12.94, and 24.94 standard cubic feet per hour), representing medium to large distribution pipeline leaks (Lamb et al., 2015). Experiments were conducted between of June 1 and 5, 2020.

A 0.08-kg hr⁻¹ leak was initiated on the first day at approximately 8:00 AM mountain daylight time, and continuous measurements were conducted over the following 24 h, at which time, the leak rate was increased to 0.18 kg hr⁻¹. This process/timing was repeated for 0.27 and 0.52 kg hr⁻¹. Mitton (2018) showed that NG released

in the METEC testbed took approximately 4 h to migrate to the surface. Therefore, only the last 20 h of data (12:00 PM–8:00 AM) were used for each of the four experiments in the analysis to allow equilibration of the subsurface and ensure steady-state conditions. To properly represent atmospheric processes at the microscale, 10-min averaged data were calculated. For every 10 min, atmospheric stability was quantified as the Obukhov length (L , m) to express the relative roles of shear and buoyancy (Foken, 2006). The Obukhov length was calculated from the surface friction velocity (u_* , m s⁻¹), the mean absolute air temperature (T , K), the von Kármán constant ($k_v = 0.41$), the gravitational acceleration ($g = 9.81$ m s⁻²), and the 3-D horizontal and vertical wind vectors (u, v, w , m s⁻¹; Equations 1 and 2; Flesch et al., 2004; Foken, 2006).

$$L = \frac{u_*^3 T}{k_v g w' T'}, \quad (1)$$

$$u_* = \left[(\overline{u'w'})^2 + (\overline{v'w'})^2 \right]^{1/4}. \quad (2)$$

The Obukhov length was converted to the PG stability class to provide practical insight for industry in situations, where on-site 3D sonic anemometer data are not available (Ulrich et al., 2019; Riddick et al., 2021). In this work, $-100 \leq L < 0$, $-500 \leq L < -100$, $|L| > 500$, $50 \leq L < 100$, and $0 < L < 50$ are considered as extremely unstable (PG: A), unstable (PG: B and C), neutral (PG: D), stable (PG: E and F), and extremely stable conditions (PG: G), respectively (Gryning et al., 2007).

2.3. Model setup

The surface CH₄ emissions were inversely calculated using WindTrax version 2.0 (Crenna, 2020). WindTrax is a publicly available backward Lagrangian stochastic-based model that can simulate the trajectories of thousands of tracer particles in the atmosphere surface layer (Flesch et al., 1995). The surface CH₄ emissions Q (kg hr⁻¹) were calculated inversely using Equation 3 by assuming the simulated normalized CH₄ mole fraction $(C/Q)_{\text{sim}}$ equals the actual normalized CH₄ mole fraction (Flesch et al., 2004)

$$Q = \frac{(C_{\text{obs}} - C_b)}{(C/Q)_{\text{sim}}}, \quad (3)$$

where C_{obs} is the measured CH₄ mole fraction (ppm) at the downwind location, and C_b is the measured local CH₄ background mole fraction (ppm). Additional details about the calculation of $(C/Q)_{\text{sim}}$ in this model can be found in Flesch et al. (2004).

Modeling inputs included CH₄ concentration, 10-min averaged wind speed and direction, air temperature, roughness length, surface expression area, and Obukhov length. The surface roughness length was estimated at 0.02 m, approximated as one-tenth of grass height (Gutmann and Small, 2005). The surface expression area was approximately 7–20 m² (**Table 1**), which was estimated using the measured surface CH₄ mole fractions (Figure S2). Atmospheric CH₄ mole fractions were filtered for two criteria: (1) the measurement was downwind of the known leak source (±90° of leak center) and (2) the

Table 2. General information about the stability sensitivity and base case in WindTrax

Baserun	Srun1	Srun2	Srun3	Srun4	Srun5	Srun6	Srun7
L	$L \times (1 - 75\%)$	$L \times (1 - 50\%)$	$L \times (1 - 25\%)$	$L \times (1 + 25\%)$	$L \times (1 + 50\%)$	$L \times (1 + 75\%)$	$L \times (1 + 100\%)$

L in the base case (Baserun) was calculated using Equations 1 and 2. The Obukhov length for the 7 sensitivity cases (Srun1–7) was –75% to 100% of L , respectively ($L \neq 0$ in WindTrax; Flesch et al., 2004); other input model parameters were the same as the Baserun.

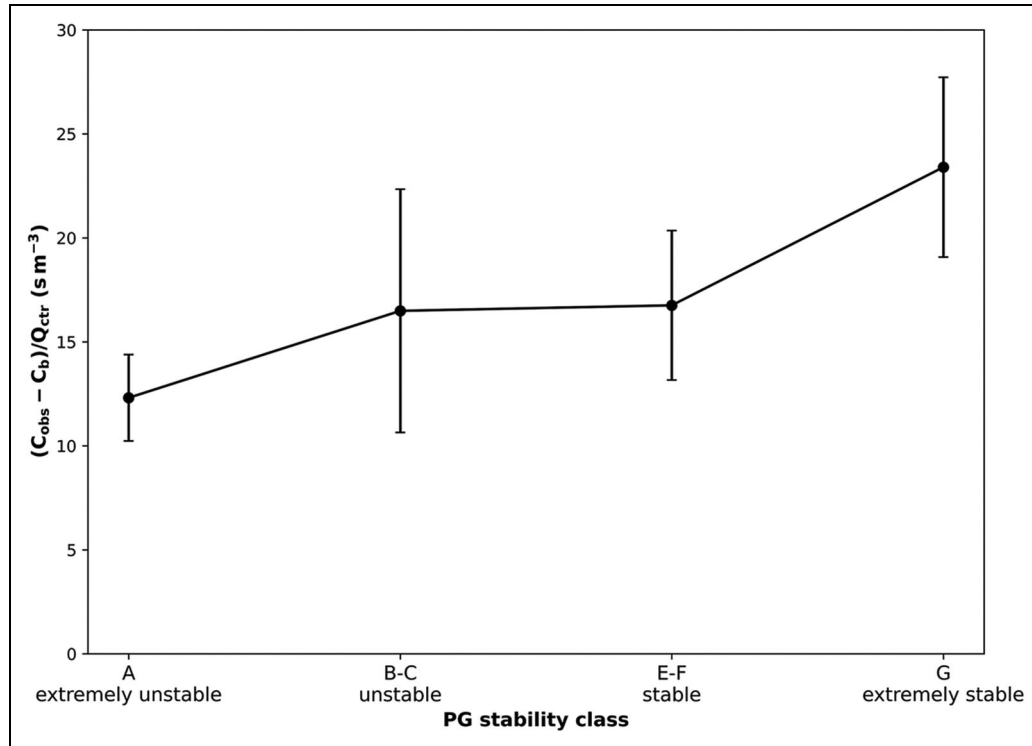


Figure 2. Mean normalized methane (CH₄) mole fraction grouped by the Pasquill–Gifford (PG) stability class for the four experiments (Experiments 1–4). C_b is the background CH₄ mole fraction (ppm), C_{obs} is the measured CH₄ mole fraction (ppm), and Q_{ctr} is the release rate (kg hr⁻¹). The error bar represents $\pm 1\sigma$ (σ : standard error). The total number of data points is 70, 10, 22, and 47 for PG stability classes A, B and C, E and F, and G, respectively. PG stability class D was not included due to limited data points (6). The averaging interval for each data point is 10 min.

CH₄ mole fraction was higher than the background CH₄ mole fraction. The background CH₄ mole fraction ranged from 1.88 to 1.92 ppm (Table 1), which was calculated by averaging the mole fraction within 25% of the cumulative distribution frequency (Figure S3).

Sensitivity analysis on seven stability cases (Srun1–7) was used to evaluate the effects of atmospheric stability on the surface CH₄ emission estimate by changing L from –75% to 100% relative to the base case (Baserun; Table 2). The base case was the controlled case in WindTrax to calculate the surface emission using 10-min averaged CH₄ mole fraction and associated meteorological variables as the model input parameters.

3. Results

3.1. Impact of atmospheric stability on CH₄ mole fraction

Figure 2 shows the mean normalized CH₄ mole fraction as a function of the PG stability class for the four

experiments (Experiments 1–4). The mean normalized CH₄ mole fractions consistently increase with the increase in atmospheric stability, ranging from 12.31 to 23.41 s m⁻³ when the atmosphere transitions from the PG stability classes A–G. The large variability in mean normalized CH₄ mole fraction may result from only measuring CH₄ mole fraction at one location within the plume for each measurement interval as well as the variations in CH₄ mole fraction within the plume for the same stability condition. The normalized CH₄ mole fraction at the plume center was larger than that at the plume edge for the same stability condition, and the normalized mole fraction near the plume centerline during the unstable condition (e.g., PG stability class A) was larger than that at the edge of the plume during the stable condition (e.g., PG stability classes E and F) (Figure S4). In all, the results confirmed that the mean normalized CH₄ mole fraction increases as the atmosphere transitions from PG stability A–G. For the conditions tested, our results show that measured CH₄

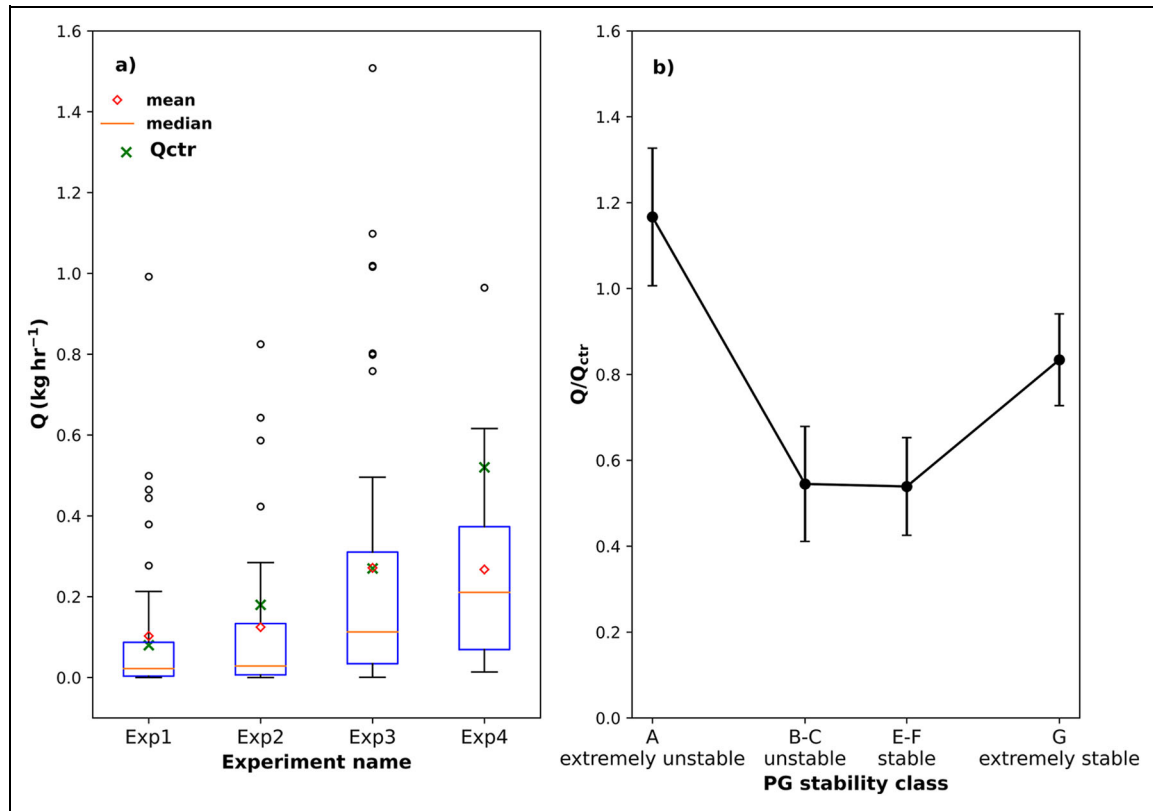


Figure 3. (a) Box and whisker plots of estimated surface methane (CH_4) emissions (Q , kg hr^{-1}) compared with the controlled release rate (Q_{ctr} , kg hr^{-1}) for the 4 controlled release experiments (Experiments 1–4). Boxes and whiskers in (a) show the median (orange), 25th and 75th percentile (blue), and minimum and maximum values (black). The mean is depicted by the hollow red diamond. The black circles represent the outliers, and the green cross-mark is the controlled release rate (Q_{ctr}). (b) The average ratio of estimated surface CH_4 emissions (Q , kg hr^{-1}) to the controlled release rate (Q_{ctr} , kg hr^{-1}) grouped by the Pasquill–Gifford (PG) stability classes. Data are from the experimental base case. The total number of data points in (b) are 70, 10, 22, and 47 for PG stability classes A, B and C, E and F, and G. PG stability class D was not included due to limited data points (6).

mole fraction cannot be used to infer the size of a leak without considering the impacts of atmospheric stability conditions.

3.2. Methane emissions calculated by WindTrax

As seen in **Figure 3a**, the model estimated surface CH_4 emissions showed large temporal variability, with the maximum estimates 3–5 times higher than the observed release rates. The absolute percentage difference between the estimated surface CH_4 emissions and the controlled release rate ranged from 1% to 48% for the four experiments (27% on average). The large absolute percentage difference in Experiment 4 may be due to the lower sample size, compared to Experiments 1–3. While Experiments 1–3 had a sample size of 6–9 h, only 3.5 h were available for Experiment 4. It is possible that the shortened time (3.5 h) is too short to accurately represent the highly temporally variable surface CH_4 emissions from a subsurface leak. Thus, the results demonstrate that for the emission rates tested, the average surface CH_4 emissions from WindTrax can provide promising estimates (within 27% on average) of the leak rate from an underground NG pipeline release based on 6.5 h of downwind measurements from a single sensor location. The average

ratio of the calculated surface CH_4 emissions by WindTrax to the controlled release rate tends to decrease with the increase in atmospheric stability except for PG stability class G, that is, a larger emission estimate during unstable conditions than in stable conditions (**Figure 3b**). The larger average ratio in PG stability class G than E and F suggests that other factors not considered in the atmospheric model, such as soil conditions, impact the surface CH_4 emissions (Cho et al., 2020; Gao et al., 2021). Previous studies have shown that temporal variability of surface CH_4 emissions is associated with both soil and atmospheric conditions, such as soil moisture and fluctuations in atmospheric pressure (Czepiel et al., 2003; Poulsen and Moldrup, 2006; Forde et al., 2019; Kim et al., 2020).

3.3. Effect of atmospheric stability on CH_4 emission estimates

Seven sensitivity cases were further used to evaluate the effect of atmospheric stability on the calculated emission rate by altering the Obukhov length in the model from -75% to 100% of L (**Table 2**). As shown in **Figure 4a**, the ratio of estimated surface CH_4 emissions to the controlled release rate decreases with the increase in atmospheric stability, where the PG stability class changes from PG

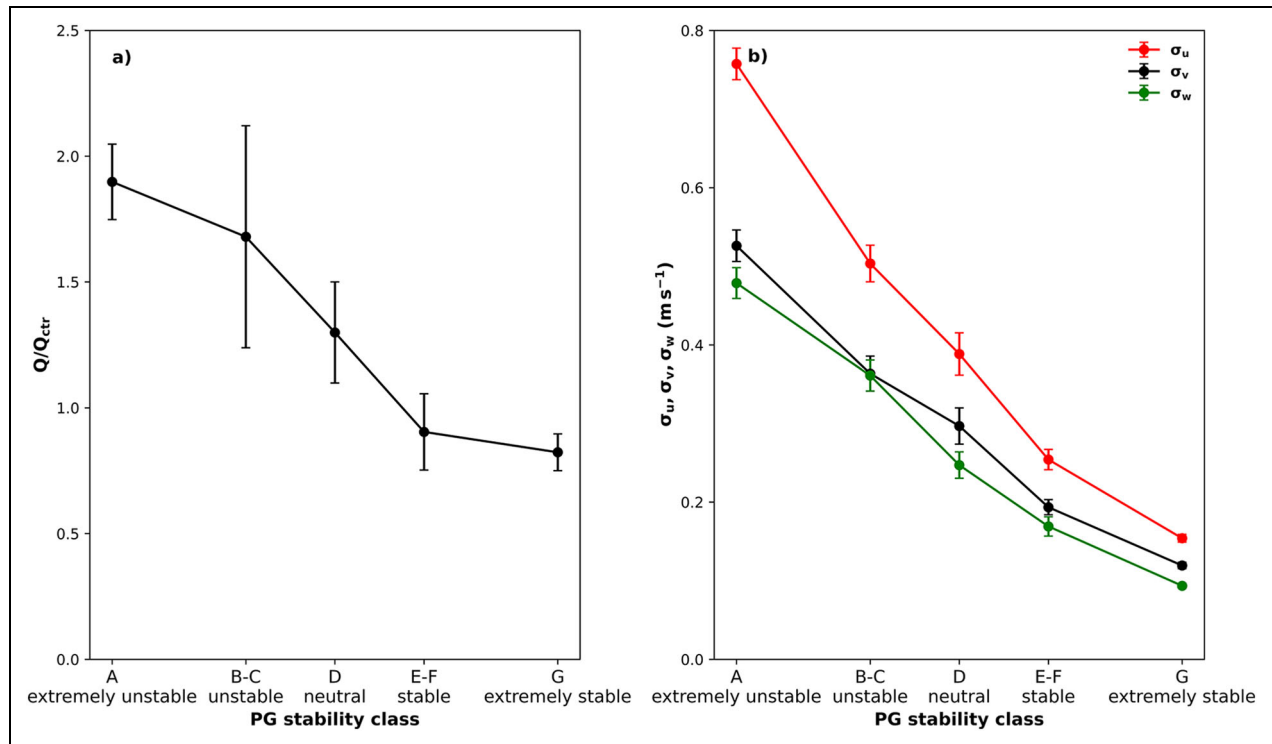


Figure 4. (a) The average ratio of estimated surface methane (CH_4) emissions (Q , $kg\ hr^{-1}$) to the controlled release rate (Q_{ctr} , $kg\ hr^{-1}$) grouped by the Pasquill–Gifford (PG) stability classes. (b) The average dispersion coefficients (σ_u : along-wind direction, σ_v : crosswind direction, and σ_w : vertical direction) grouped by the PG stability class. The unit of dispersion coefficient is $m\ s^{-1}$. The data in (a) and (b) are from the sensitivity cases, as shown in **Table 2**. The error bars in (a) and (b) represent $\pm 1\sigma$ (σ : standard error). The total number of data points are 326, 91, 58, 191, and 355 for PG stability classes A, B and C, D, E and F, and G, respectively.

stability class A (extremely unstable) to G (extremely stable). As the atmosphere transitions from A to G, the average dispersion coefficients of the along-wind, crosswind, and vertical direction decrease rapidly (**Figure 4b**). The dispersion coefficient in the 3-D direction is about 0.4–0.8 $m\ s^{-1}$ when the atmosphere is in PG stability class A (extremely unstable), but it reduces to below 0.2 in PG stability class G (extremely stable, a 50%–70% decrease). Thus, the strong dispersion during unstable atmospheric conditions results in enhanced vertical and horizontal mixing compared to the inhibited dispersion and hence mixing during stable conditions (Riddle et al., 2004; Leelóssy et al., 2014). This results in broad yet diluted CH_4 plume during unstable conditions (e.g., PG stability class A) and narrow yet concentrated CH_4 plume during stable conditions (e.g., PG stability classes E and F; Figure S4).

3.4. Effect of time averaging on CH_4 emission estimates

Using the estimated emissions from the base case (Base-run), a rolling mean method was used to understand the amount of downwind data needed over time to accurately estimate the emission rate. Although our experiments collected data for 24 h, in field scenarios, this is often not possible. We therefore wanted to understand the effect of time averaging on the emission estimate. **Figure 5** shows the probability that the emission estimate is within $\pm 50\%$

of the controlled release rate ($P_{\pm 50\%}$) for data averaging time of 0.33–9.33 h. As expected, the probability increases with the increase in the rolling mean time in Experiments 1 through 3 (**Figure 5**). A probability of 50% is achieved when approximately 1 h of data is collected. The probability increases to 80% with about 2 h of data and reaches 100% with 3–4 h of data. However, the probability was not observed to increase with an increase in time in Experiment 4 (**Figure 5**). This may be due to the smaller sample size (3.5 h of downwind data in Experiment 4) and its distribution characteristics. As shown in **Figure 3a**, the distribution was normal for Experiment 4 but was right-skewed for Experiments 1–3. Despite this, it should be acknowledged that the low sample size for Experiment 4 may have affected the probability.

4. Discussion

This work demonstrates the viability of linking a simple publicly available dispersion model with limited above-ground and surface CH_4 mole fraction and micrometeorological data to estimate CH_4 emissions from underground pipeline leaks. Previous downwind methods used for aboveground NG infrastructure leaks show that emission estimate accuracy is about $\pm 70\%$ when calculating based on 15–20 min of downwind stationary measurements (Heltzel et al., 2020). For belowground CH_4 leaks, our method shows that downwind measurements measured over 4 h can be used to estimate a leak between 0.08 and

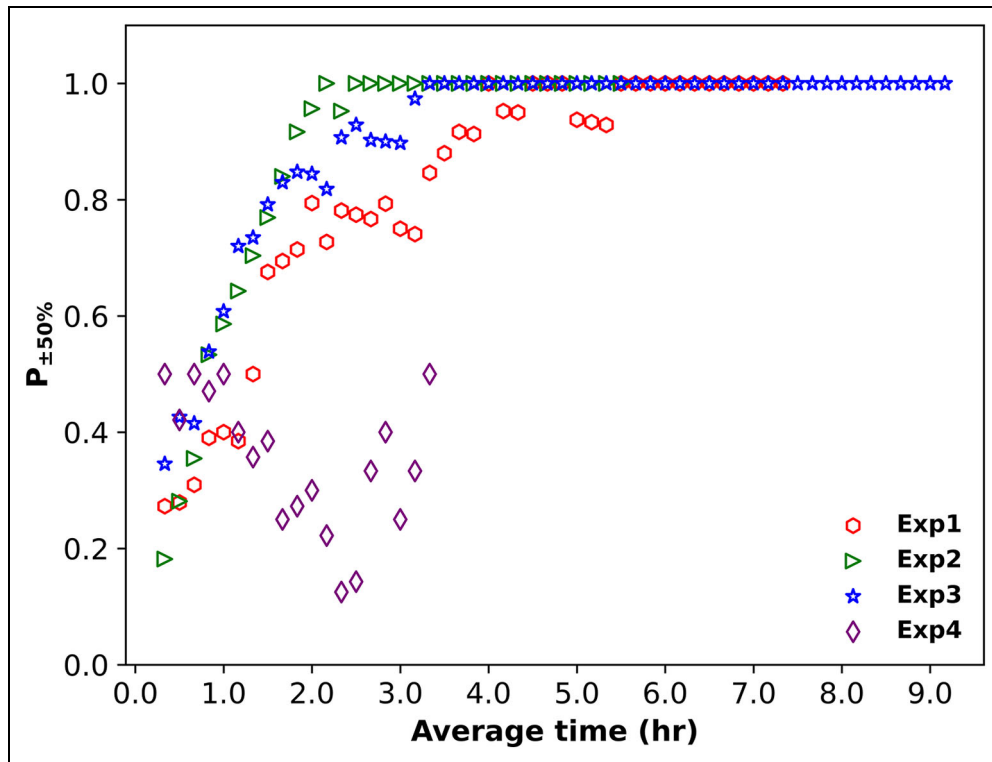


Figure 5. Probability ($P_{\pm 50\%}$) that the calculated mean methane (CH_4) emissions (Q , kg hr^{-1}) is within $\pm 50\%$ of the controlled release rate (Q_{ctr} , kg hr^{-1}) with the rolling mean time ranging from 0.33 to 9.33 h. The data were individual surface CH_4 emission points from the base case (Baserun). The probability was calculated by dividing the number of emission estimates within $\pm 50\%$ of the controlled release rate by the total sample size in each rolling time interval.

0.52 kg h^{-1} to within $\pm 50\%$ in an open field condition. Although the average CH_4 emissions calculated by WindTrax showed good agreement with the controlled release rate, we also recognize that it might not be feasible to directly apply this method to estimate emissions from a large number of pipeline leaks (U.S. Energy Information Administration, 2021). However, this method could be modified to vehicle-based surveys using a gas sensor and associated 3-D anemometer data to extend its applicability. The method presented here is similar to the survey protocols outlined in other mobile methods for NG aboveground infrastructure leaks (Brantley et al., 2014; Caulton et al., 2018; Edie et al., 2020), that is, mobile monitoring and downwind stationary CH_4 mole fraction measurements, yet demonstrates the importance of providing enough data over time for proper estimation of belowground leak scenarios. The length of time needed for mobile methods to achieve an equivalent accuracy remains unknown as there are currently no controlled belowground experiments results for mobile methods. The reported large emission estimate uncertainty (between -50% and $+350\%$) of mobile methods on aboveground NG infrastructure leaks suggests more mobile transects are needed to improve the emission estimate (Lan et al., 2015; Rella et al., 2015; Yacovitch et al., 2015). A driving measurement campaign by Caulton et al. (2018) shows that at least 10 repeat transects are needed to reduce uncertainty, where the uncertainty is estimated at 0.05–6.5 times the emission rate for single-transect

sites and 0.5–2.7 times the emission rate for sites with more than 10 transects. Therefore, Caulton's emphasis on more transect time may also apply to the mobile methods for improving emission accuracy from pipeline leaks.

There is limited information regarding emissions from both flow and gathering lines (Zimmerle et al., 2017; Li et al., 2020). The emission factors of NG gathering lines in the current U.S. Environmental Protection Agency Greenhouse Gas Inventory (Hockstad and Hanel, 2018) are based on emission estimates from the distribution pipelines (Campbell et al., 1996). With enhanced mobility, the method presented here shows potential for estimating CH_4 emissions from NG flow and gathering lines. Similarly, it is also useful for NG distribution and transmission pipeline operators when an accurate estimate of emission rate is required to inform the priority of leak repairs, such as finding and repairing the largest leaks and prioritizing work schedules.

5. Conclusions

This work tests an approach to estimate CH_4 emission rates compared to known leak rates from subsurface pipeline leaks under realistic conditions. Our results confirm that the mean normalized CH_4 mole fraction increases as the atmosphere transitions from PG stability classes A–G. The measured CH_4 mole fraction cannot be used to infer the size of a leak without considering the impacts of atmospheric stability conditions. The estimated CH_4 surface emissions from a simple publicly available

dispersion model showed large temporal variability, and for the emission rates tested, at least 6 h of data are needed to have a representative estimate from subsurface pipeline leaks ($\pm 27\%$ of the controlled release rate on average). The probability that the emission estimate is within $\pm 50\%$ of the controlled release rate ($P_{\pm 50\%}$) is about 50% when approximately 1 h of data is collected. Probability increases to 80% with about 2 h of data and reaches 100% with 3–4 h of data. A sensitivity analysis also showed that the estimated surface CH₄ emissions from the underground leaks tend to decrease when the atmosphere transitions from the PG stability class A (extremely unstable) to G (extremely stable) due to the inhibited dispersion and mixing in the atmosphere.

These findings of this study emphasize that a certain amount of data are necessary to have an estimate that can reflect the true subsurface leak rates. Atmospheric stability conditions should be incorporated in pipeline emission estimates based on the atmospheric CH₄ measurements.

Data accessibility statement

Data sets for this research are available in the in-text data citation reference: Tian, Shanru; Smits, Kathleen M.; Cho, Younki; Riddick, Stuart; Zimmerle, Daniel; Duggan, Aidan. 2022. Replication data for estimating methane emissions from underground natural gas pipelines using an atmospheric dispersion-based method, <https://doi.org/10.18738/T8/UAO5XX>, Texas Data Repository.

Supplemental files

The supplemental files for this article can be found as follows:

Figures S1–S4. (DOC)

Acknowledgments

Any opinion, findings, conclusions, or recommendations expressed here are those of the authors and do not necessarily reflect the views of those providing technical input or financial support. The trade names mentioned here are merely for identification purposes and do not constitute an endorsement by any entity involved in this study. The authors also thank Timothy Vaughn and Clay Bell for their experimental support.

Funding

This work is jointly supported by the U.S. Department of Transportation Pipeline and Hazardous Materials Safety Administration under Grant Nos. 693JK31810013 and 693JK32010011 and by the Colorado Oil and Gas Conservation Commission Mark Martinez & Joey Irwin Memorial Public Projects Fund.

Competing interests

The authors declare no competing financial interest.

Author contributions

Contributed to conception and design: ST, KS, YC, SR, DZ. Contributed to the acquisition of data: SR, AD.

Contributed to analysis and interpretation of data: ST, KS, YC, SR.

Drafted and/or revised the article: ST, KS, YC, SR, DZ, AD.

Approved the submitted version for publication: ST, KS, YC, SR, DZ, AD.

References

- Alvarez, RA, Pacala, SW, Winebrake, JJ, Chameides, WL, Hamburg, SP.** 2012. Greater focus needed on methane leakage from natural gas infrastructure. *Proceedings of the National Academy of Sciences of the United States of America* **109**(17): 6435–6440. DOI: <https://doi.org/10.1073/pnas.1202407109>.
- Barkley, ZR, Lauvaux, T, Davis, KJ, Deng, A, Miles, NL, Richardson, SJ, Cao, Y, Sweeney, C, Karion, A, Smith, M, Kort, EA, Schwietzke, S, Murphy, T, Cervone, G, Martins, D, Maasackers, JD.** 2017. Quantifying methane emissions from natural gas production in north-eastern Pennsylvania. *Atmospheric Chemistry and Physics* **17**(22): 13941–13966. DOI: <https://doi.org/10.5194/acp-17-13941-2017>.
- Bonifacio, HF, Maghirang, RG, Razote, EB, Trabue, SL, Prueger, JH.** 2013. Comparison of AERMOD and WindTrax dispersion models in determining PM10 emission rates from a beef cattle feedlot. *Journal of the Air & Waste Management Association* **63**(5): 545–556. DOI: <https://doi.org/10.1080/10962247.2013.768311>.
- Brantley, HL, Thoma, ED, Squier, WC, Guven, BB, Lyon, D.** 2014. Assessment of methane emissions from oil and gas production pads using mobile measurements. *Environmental Science & Technology* **48**(24): 14508–14515. DOI: <https://doi.org/10.1021/es503070q>.
- Campbell, LM, Campbell, MV, Epperson, D.** 1996. *Methane emissions from the natural gas industry volume 9: Underground pipelines*. Washington, DC: U.S. Environmental Protection Agency. EPA/600/R-96/080i (NTIS PB97-143002). Available at https://cfpub.epa.gov/si/si_public_record_report.cfm?Lab=NRMRL&dirEntryId=115618. Accessed February 5, 2022.
- Caulton, DR, Li, Q, Bou-Zeid, E, Fitts, JP, Golston, LM, Pan, D, Lu, J, Lane, HM, Buchholz, B, Guo, X, McSpirtt, J, Wendt, L, Zondlo, MA.** 2018. Quantifying uncertainties from mobile-laboratory-derived emissions of well pads using inverse Gaussian methods. *Atmospheric Chemistry and Physics* **18**(20): 15145–15168. DOI: <https://doi.org/10.5194/acp-18-15145-2018>.
- Cho, Y, Smits, KM, Riddick, SN, Zimmerle, DJ.** 2022. Calibration and field deployment of low-cost sensor network to monitor underground pipeline leakage. *Sensors and Actuators B: Chemical* **355**: 131276. DOI: <https://doi.org/10.1016/j.snb.2021.131276>.
- Cho, Y, Ulrich, BA, Zimmerle, DJ, Smits, KM.** 2020. Estimating natural gas emissions from underground pipelines using surface concentration measurements☆.

- Environmental Pollution* **267**: 115514. DOI: <https://doi.org/10.1016/j.envpol.2020.115514>.
- Crenna, B.** 2020. An introduction to WindTrax. Available at <http://www.thunderbeachscientific.com>. Accessed May 2, 2022.
- Czepiel, PM, Shorter, JH, Mosher, B, Allwine, E, McManus, JB, Harriss, RC, Kolb, CE, Lamb, BK.** 2003. The influence of atmospheric pressure on landfill methane emissions. *Waste Management* **23**(7): 593–598. DOI: [https://doi.org/10.1016/S0956-053X\(03\)00103-X](https://doi.org/10.1016/S0956-053X(03)00103-X).
- Defratyka, SM, Paris, JD, Yver-Kwok, C, Fernandez, JM, Korben, P, Bousquet, P.** 2021. Mapping urban methane sources in Paris, France. *Environmental Science & Technology* **55**(13): 8583–8591. DOI: <https://doi.org/10.1021/acs.est.1c00859>.
- Edie, R, Robertson, AM, Field, RA, Soltis, J, Snare, DA, Zimmerle, D, Bell, CS, Vaughn, TL, Murphy, SM.** 2020. Constraining the accuracy of flux estimates using OTM 33A. *Atmospheric Measurement Techniques* **13**(1): 341–353. DOI: <https://doi.org/10.5194/amt-13-341-2020>.
- Flesch, TK, Wilson, JD, Harper, LA, Crenna, BP, Sharpe, RR.** 2004. Deducing ground-to-air emissions from observed trace gas concentrations: A field trial. *Journal of Applied Meteorology and Climatology* **43**(3): 487–502. DOI: [https://doi.org/10.1175/1520-0450\(2004\)043<0487:DGEFOT>2.0.CO;2](https://doi.org/10.1175/1520-0450(2004)043<0487:DGEFOT>2.0.CO;2).
- Flesch, TK, Wilson, JD, Yee, E.** 1995. Backward-time Lagrangian stochastic dispersion models and their application to estimate gaseous emissions. *Journal of Applied Meteorology and Climatology* **34**(6): 1320–1332. DOI: [https://doi.org/10.1175/1520-0450\(1995\)034<1320:BTLSDM>2.0.CO;2](https://doi.org/10.1175/1520-0450(1995)034<1320:BTLSDM>2.0.CO;2).
- Foken, T.** 2006. 50 Years of the Monin–Obukhov similarity theory. *Boundary-Layer Meteorology* **119**(3): 431–447. DOI: <https://doi.org/10.1007/s10546-006-9048-6>.
- Forde, ON, Cahill, AG, Beckie, RD, Mayer, KU.** 2019. Barometric-pumping controls fugitive gas emissions from a vadose zone natural gas release. *Scientific Reports* **9**(1): 1–9. DOI: <https://doi.org/10.1038/s41598-019-50426-3>.
- Gallagher, ME, Down, A, Ackley, RC, Zhao, K, Phillips, N, Jackson, RB.** 2015. Natural gas pipeline replacement programs reduce methane leaks and improve consumer safety. *Environmental Science & Technology Letters* **2**(10): 286–291. DOI: <https://doi.org/10.1021/acs.estlett.5b00213>.
- Gao, B, Mitton, MK, Bell, C, Zimmerle, D, Deepagoda, TKKC, Hecobian, A, Smits, KM.** 2021. Study of methane migration in the shallow subsurface from a gas pipe leak. *Elementa: Science of the Anthropocene* **9**: 1. DOI: <https://doi.org/10.1525/elementa.2021.00008>.
- Gryning, SE, Batchvarova, E, Brümmer, B, Jørgensen, H, Larsen, S.** 2007. On the extension of the wind profile over homogeneous terrain beyond the surface boundary layer. *Boundary-Layer Meteorology* **124**(2): 251–268. DOI: <https://doi.org/10.1007/s10546-007-9166-9>.
- Gutmann, ED, Small, EE.** 2005. The effect of soil hydraulic properties vs. soil texture in land surface models. *Geophysical Research Letters* **32**(2): 1–4. DOI: <https://doi.org/10.1029/2004GL021843>.
- Heltzel, RS, Zaki, MT, Gebreslase, AK, Abdul-Aziz, OI, Johnson, DR.** 2020. Continuous otm 33A analysis of controlled releases of methane with various time periods, data rates and wind filters. *Environments* **7**(9): 65. DOI: <https://doi.org/10.3390/environments7090065>.
- Hendrick, MF, Ackley, R, Sanaie-Movahed, B, Tang, X, Phillips, NG.** 2016. Fugitive methane emissions from leak-prone natural gas distribution infrastructure in urban environments. *Environmental Pollution* **213**: 710–716. Amsterdam, The Netherlands: Elsevier Ltd. DOI: <https://doi.org/10.1016/j.envpol.2016.01.094>.
- Hockstad, L, Hanel, L.** 2018. *Inventory of U.S. greenhouse gas emissions and sinks (No. cdiac: EPA-EMISSIONS)*. Environmental System Science Data Infrastructure for a Virtual Ecosystem. DOI: <https://doi.org/10.15485/1464240>.
- Intergovernmental Panel on Climate Change.** 2014. Anthropogenic and natural radiative forcing. In *Climate change 2013—The physical science basis: Working Group I contribution to the Fifth Assessment Report of the Intergovernmental Panel on Climate Change*. Cambridge UK: Cambridge University Press: 659–740. DOI: <https://doi.org/10.1017/CBO9781107415324.018>.
- Jeong, SJ.** 2011. CALPUFF and AERMOD dispersion models for estimating odor emissions from industrial complex area sources. *Asian Journal of Atmospheric Environment* **5**(1): 1–7. DOI: <https://doi.org/10.5572/ajae.2011.5.1.001>.
- Kim, H, Yun, S, Han, SH, Son, Y, Kim, S, Ko, D.** 2020. Real-time monitoring of carbon dioxide emissions from a shallow carbon dioxide release experiment. *Vadose Zo Journal* **19**: e20051. DOI: <https://doi.org/10.1002/vzj2.20051>.
- Lamb, BK, Edburg, SL, Ferrara, TW, Howard, T, Harrison, MR, Kolb, CE, Townsend-Small, A, Dyck, W, Possolo, A, Whetstone, JR.** 2015. Direct measurements show decreasing methane emissions from natural gas local distribution systems in the United States. *Environmental Science & Technology* **49**(8): 5161–5169. DOI: <https://doi.org/10.1021/es505116p>.
- Lan, X, Talbot, R, Laine, P, Torres, A.** 2015. Characterizing fugitive methane emissions in the Barnett shale area using a mobile laboratory. *Environmental Science & Technology* **49**(13): 8139–8146. DOI: <https://doi.org/10.1021/es5063055>.
- Laubach, J, Kelliher, FM.** 2005. Methane emissions from dairy cows: Comparing open-path laser measurements to profile-based techniques. *Agricultural and Forest Meteorology* **135**(1–4): 340–345. DOI: <https://doi.org/10.1016/j.agrformet.2005.11.014>.

- Leelőssy, Á, Molnár, F, Izsák, F, Havasi, Á, Lagzi, I, Mészáros, R.** 2014. Dispersion modeling of air pollutants in the atmosphere: A review. *Central European Journal of Geosciences* **6**(3): 257–278. DOI: <https://doi.org/10.2478/s13533-012-0188-6>.
- Li, HZ, Mundia-Howe, M, Reeder, MD, Pekney, NJ.** 2020. Gathering pipeline methane emissions in utica shale using an unmanned aerial vehicle and ground-based mobile sampling. *Atmos* **11**(7): 1–13. DOI: <https://doi.org/10.3390/atmos11070716>.
- Mitton, M.** 2018. Subsurface methane migration from natural gas distribution [MS thesis]. Golden, CO: Colorado School of Mines, Dept. of Civil and Environmental Engineering. Available at https://repository.mines.edu/bitstream/handle/11124/172530/Mitton_mines_0052N_11576.pdf?sequence=1&isAllowed=y. Accessed May 2, 2022.
- Mønster, J, Kjeldsen, P, Scheutz, C.** 2019. Methodologies for measuring fugitive methane emissions from landfills—A review. *Waste Management* **87**: 835–859. DOI: <https://doi.org/10.1016/j.wasman.2018.12.047>.
- National Academies of Sciences, EM.** 2018. *Improving characterization of anthropogenic methane emissions in the United States*. Washington, DC: The National Academies Press. DOI: <https://doi.org/10.17226/24987>.
- National Association of Regulatory Utility Commissioners.** 2019. Sampling of methane emissions detection technologies and practices for natural gas distribution infrastructure. Available at <https://pubs.naruc.org/pub/OCA39FB4-A38C-C3BF-5B0A-FCD60A7B3098>. Accessed May 2, 2022.
- Okamoto, H, Gomi, Y.** 2011. Empirical research on diffusion behavior of leaked gas in the ground. *Journal of Loss Prevention in the Process Industries* **24**(5): 531–540. DOI: <https://doi.org/10.1016/j.jlp.2011.01.007>.
- Pipeline and Hazardous Materials Safety Administration.** 2017. Guidance manual for operators of small natural gas systems. Available at <https://www.phmsa.dot.gov/training/pipeline/small-natural-gas-operator-guide-january-2017-pdf>. Accessed May 2, 2022.
- Pipeline and Hazardous Materials Safety Administration.** 2018. Pipeline failure causes. Available at <https://www.phmsa.dot.gov/incident-reporting/accident-investigation-division/pipeline-failure-causes>. Accessed May 2, 2022.
- Pipeline and Hazardous Materials Safety Administration.** 2022. SIGNIFICANT INCIDENT 20 YEAR TREND. Available at <https://www.phmsa.dot.gov/data-and-statistics/pipeline/pipeline-incident-20-year-trends>. Accessed April 24, 2022.
- Poulsen, TG, Møldrup, P.** 2006. Evaluating effects of wind-induced pressure fluctuations on soil-atmosphere gas exchange at a landfill using stochastic modelling. *Waste Management & Research* **24**(5): 473–481. DOI: <https://doi.org/10.1177/0734242X06066363>.
- Rella, CW, Tsai, TR, Botkin, CG, Crosson, ER, Steele, D.** 2015. Measuring emissions from oil and natural gas well pads using the mobile flux plane technique. *Environmental Science & Technology* **49**(7): 4742–4748. DOI: <https://doi.org/10.1021/acs.est.5b00099>.
- Riddick, SN, Bell, CS, Duggan, A, Vaughn, TL, Smits, KM, Cho, Y, Bennett, KE, Zimmerle, DJ.** 2021. Modeling temporal variability in the surface expression above a methane leak: The ESCAPE model. *Journal of Natural Gas Science and Engineering* **96**: 104275. DOI: <https://doi.org/10.1016/j.jngse.2021.104275>.
- Riddick, SN, Hancock, BR, Robinson, AD, Connors, S, Davies, S, Allen, G, Pitt, J, Harris, NRP.** 2018. Development of a low-maintenance measurement approach to continuously estimate methane emissions: A case study. *Waste Management* **73**: 210–219. DOI: <https://doi.org/10.1016/j.wasman.2016.12.006>.
- Riddick, SN, Mauzerall, DL, Celia, M, Harris, NRP, Allen, G, Pitt, J, Staunton-Sykes, J, Forster, GL, Kang, M, Lowry, D, Nisbet, EG, Manning, AJ.** 2019. Measuring methane emissions from oil and gas platforms in the North Sea. *Atmospheric Chemistry and Physics, Discussions* **19**(15): 9787–9796. DOI: <https://doi.org/10.5194/acp-2019-90>.
- Riddick, SN, Mauzerall, DL, Celia, MA, Kang, M, Bandilla, K.** 2020. Variability observed over time in methane emissions from abandoned oil and gas wells. *International Journal of Greenhouse Gas Control* **100**: 103116. DOI: <https://doi.org/10.1016/j.ijggc.2020.103116>.
- Riddle, A, Carruthers, D, Sharpe, A, McHugh, C, Stocker, J.** 2004. Comparisons between FLUENT and ADMS for atmospheric dispersion modelling. *Atmospheric Environment* **38**(7): 1029–1038. DOI: <https://doi.org/10.1016/j.atmosenv.2003.10.052>.
- Ulrich, BA, Mitton, M, Lachenmeyer, E, Hecobian, A, Zimmerle, D, Smits, KM.** 2019. Natural gas emissions from underground pipelines and implications for leak detection. *Environmental Science & Technology Letters* **6**(7): 401–406. DOI: <https://doi.org/10.1021/acs.estlett.9b00291>.
- United Nations Framework Convention on Climate Change.** 2022. The Paris agreement. Available at <https://unfccc.int/process-and-meetings/the-paris-agreement/the-paris-agreement>. Accessed May 2, 2022.
- U.S. Energy Information Administration.** 2021. Natural gas explained: Natural gas pipelines. Available at <https://www.eia.gov/energyexplained/natural-gas/natural-gas-pipelines.php>. Accessed May 2, 2022.
- Von Fischer, JC, Cooley, D, Chamberlain, S, Gaylord, A, Griebenow, CJ, Hamburg, SP, Salo, J, Schumacher, R, Theobald, D, Ham, J.** 2017. Rapid, vehicle-based identification of location and magnitude of urban natural gas pipeline leaks. *Environmental Science & Technology* **51**(7): 4091–4099. DOI: <https://doi.org/10.1021/acs.est.6b06095>.
- Washington Administrative Code.** 2019. Leak classification and action criteria. Available at <https://apps>.

leg.wa.gov/WAC/default.aspx?cite=480-93-18601. Accessed May 2, 2022.

Weller, ZD, Hamburg, SP, Von Fischer, JC. 2020. A national estimate of methane leakage from pipeline mains in natural gas local distribution systems. *Environmental Science & Technology* **54**(14): 8958–8967. DOI: <https://doi.org/10.1021/acs.est.0c00437>.

Weller, ZD, Roscioli, JR, Daube, WC, Lamb, BK, Ferrara, TW, Brewer, PE, Von Fischer, JC. 2018. Vehicle-based methane surveys for finding natural gas leaks and estimating their size: Validation and uncertainty. *Environmental Science & Technology* **52**(20): 11922–11930. DOI: <https://doi.org/10.1021/acs.est.8b03135>.

Yacovitch, TI, Herndon, SC, Pétron, G, Kofler, J, Lyon, D, Zahniser, MS, Kolb, CE. 2015. Mobile laboratory

observations of methane emissions in the Barnett shale region. *Environmental Science & Technology* **49**(13): 7889–7895. DOI: <https://doi.org/10.1021/es506352j>.

Yang, W, Zhu, A, Zhang, J, Xin, X, Zhang, X. 2017. Evaluation of a backward Lagrangian stochastic model for determining surface ammonia emissions. *Agricultural and Forest Meteorology* **234**: 196–202. DOI: <https://doi.org/10.1016/j.agrformet.2017.01.001>.

Zimmerle, DJ, Pickering, CK, Bell, CS, Heath, GA, Nummedal, D, Pétron, G, Vaughn, TL. 2017. Gathering pipeline methane emissions in Fayetteville shale pipelines and scoping guidelines for future pipeline measurement campaigns. *Elementa: Science of the Anthropocene* **5**: 70. DOI: <https://doi.org/10.1525/elementa.258>.

How to cite this article: Tian, S, Smits, KM, Cho, Y, Riddick, SN, Zimmerle, DJ, Duggan, A. 2022. Estimating methane emissions from underground natural gas pipelines using an atmospheric dispersion-based method. *Elementa: Science of the Anthropocene* 10(1). DOI: <https://doi.org/10.1525/elementa.2022.00045>

Domain Editor-in-Chief: Detlev Helmig, Boulder AIR LLC, Boulder, CO, USA

Guest Editor: Brian Lamb, Washington State University, Pullman, WA, USA

Knowledge Domain: Atmospheric Science

Published: August 29, 2022 **Accepted:** July 13, 2022 **Submitted:** March 14, 2022

Copyright: © 2022 The Author(s). This is an open-access article distributed under the terms of the Creative Commons Attribution 4.0 International License (CC-BY 4.0), which permits unrestricted use, distribution, and reproduction in any medium, provided the original author and source are credited. See <http://creativecommons.org/licenses/by/4.0/>.

